LUND UNIVERSITY

Tissue temperature measurements during interstitial laser therapy using Cr^{3+}-doped crystals at the fiber tip

Svensson, Jenny; Ralsgard, Anna; Johansson, Thomas; Andersson-Engels, Stefan

Link to publication

Tissue temperature measurements during interstitial laser therapy using Cr^{3+}-doped crystals at the fiber tip

J. Svensson, A. Ralsgård, T. Johansson, S. Andersson-Engels

Lund University Medical Laser Centre, Department of Physics, Lund Institute of Technology,
P.O. Box 118, SE-221 00 Lund, Sweden. +46 46 222 31 19

ABSTRACT

In this project a technique to optically measure the temperature is evaluated. The measurement is to be performed through optical fibres during photodynamic laser treatments or laser thermo therapy of malignant tumours. For this technique Cr^{3+}-doped crystals were used. The lifetime of the ions' fluorescence were measured, since the fluorescence is strongly temperature dependent. A piece of a crystal was attached to the tip of an optical fibre. The crystal was excited at 635 nm, which is the wavelength most frequently used for photodynamic treatment.

An accuracy in the temperature measurement of ± 0.3 °C was obtained for Cr:LiSAF in the region 20 – 70 °C. This is well within the requirements for this application. Alexandrite and Cr:YAG were also evaluated in this study, also yielding a very good accuracy. A laser treatment was simulated using pork chop as tissue phantom and the temperature was measured.

Keywords: Temperature-dependent fluorescence, Cr^{3+}-ions

1. INTRODUCTION

The aim of this project was to evaluate an optical technique to measure the temperature in the tissue, during interstitial photodynamic therapy (IPDT) treatment [1,2] or laser thermo therapy of malignant tumours.[3] During an IPDT treatment, fibres are inserted into the tumour. Laser light guided through these fibres induces tumour cell death together with a tumour marker, e.g. Protophorfyrin IX (PpIX). If a local bleeding occurs close to the fibre tip, the temperature will increase due to the higher absorption of light in blood. The high absorption will reduce the efficiency of the treatment. Therefore, it would be favourable if the temperature could be monitored, so the treatment can be optimised and the outcome accurately predicted. [4,5]

Preferably one would like to be able to measure the temperature with the same fibres that delivers the light during the treatment. A possible way to do this is to attach a crystal, whose fluorescence is temperature dependent, to the fibre tip. Some requirements are that it should be possible to excite the crystal at the treatment wavelength, 635 nm, and that the fluorescence induced in the crystal is sensitive to temperatures in the region 20 – 70 °C, because this temperature interval is interesting for the applications. When doing experiments with tissue phantoms, it is necessary to be able to measure down to room temperature and in laser thermo therapy temperatures up to at least 70 °C must be measurable. The accuracy required is approximately 1 °C in order to predict treatment results. An advantage would be if the fluorescence spectrum from the crystal easily could be separated from tissue autofluorescence. It is also desirable that the crystal should not absorb light around 405 nm, to prevent interference with the PpIX fluorescence measurements during an IPDT treatment.

1.1   Cr^{3+}-doped materials

Cr^{3+}-ions in ionic crystals interact strongly with the crystal field and the lattice vibrations. The crystal field arises because of the influence on the Cr^{3+}-ion from the neighbouring ions. The interaction between the Cr^{3+}-ions and the crystal field arises due to the fact that there are no outer shells to shield the three valence electrons. As a result Cr^{3+}-activated materials are characterised by a wide absorption spectrum, from UV to infrared. This has two advantages, the possibility to choose excitation source and that a small drift in the excitation source will not cause a significant change in fluorescence intensity. Because of the strong crystal field interaction, the energy gaps of the electronic levels of Cr^{3+} can vary from one host crystal to another. The temperature dependence of the fluorescence lifetime varies with the energy

gap and will thus differ for different Cr^{3+}-doped materials. To measure the temperature using the fluorescence signal from a Cr^{3+}-doped crystal, the type of crystal should thus be selected with respect to the temperature interval of interest.[6]

The ground state in Cr^{3+} is always $^4A_2$, independent of the strength of the crystal field. Two excited energy levels are involved, following excitation at 635 nm: $^4T_2$ and ^2E. The energy splitting between these two low-lying states is denoted $\Delta E = E(^4T_2) - E(^2E)$. ΔE varies strongly with the strength of the crystal field and can be both negative and positive. At high crystal field strength, for example in ruby, Cr:YAG and alexandrite, ΔE is positive and the emission of the Cr^{3+} is dominated by the transition, $^2E \rightarrow {}^4A_2$. In low crystal field strength, for example in Cr:LiSAF, the dominating transition is $^4T_2 \rightarrow {}^4A_2$. [6]

The emission spectrum of Cr^{3+} consists of two different features, a broad spectral band and two sharp peaks, so called R-lines. The broad band originates from the vibronic transitions, $^4T_2 \rightarrow {}^4A_2$, where ions in the $^4T_2$ state decay to the empty vibrational levels of the $^4A_2$ state. The R-lines appear because of the further split of the ^2E state into two levels, E and $2\bar{A}$, separated by a small energy gap. The R_1-line is the transition $E \rightarrow {}^4A_2$ and the R_2-line comes from the transition $2\bar{A} \rightarrow {}^4A_2$. [6]

Lattice vibrations in the crystal interact with the electronic levels of the Cr^{3+}-ion. The effects of this are the initiation of vibronic transitions, radiationless transitions and phonon scattering. The first of these effects produces broad bands in the spectra, the second effect leads to a temperature dependent decrease of the fluorescence lifetimes of the R-lines and both the second and third effect can cause a thermal broadening of the R-lines.[7]

1.1.1 Low crystal field strength

In low crystal field strength, the transition $^4T_2 \rightarrow {}^4A_2$ occurs through two processes, one is the radiative transition initiated from I seen in Figure 1. The other is a nonradiative process due to thermal quenching of the Cr^{3+}-ions. Some ions will be thermally elevated to Q, which is the energy crossing between the excited state and the ground state. These ions will decay to the ground state and will there undergo stepwise transitions to the lowest level of the ground state through nonradiative relaxation. These two processes compete with each other constantly.[6]
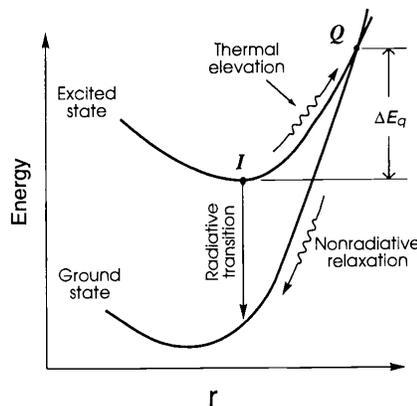
Figure 1. Energy levels as a function of nearest neighbour distance
for crystals with a low crystal field strength[6]

When the temperature increases (above 275 K), more excited ions will be elevated to Q, due to the larger neighbour distance, and the nonradiative process, called quenching, will become stronger. Normally, the nonradiative transitions have a shorter lifetime resulting in a decrease in the observed fluorescence lifetime with increasing temperature. The fluorescence intensity will decrease with increasing temperature due to an increase in the fraction of ions deexcited through nonradiative transitions.[6]

The impact of the ^2E state on the fluorescence lifetime is negligible. This is partly due to the low population of the ^2E state according to the Boltzmann distribution and partly due to that the transition $^2E \rightarrow {}^4A_2$ is forbidden both by parity and spin. The transition rate is thus one or two orders of magnitude lower than the transition $^4T_2 \rightarrow {}^4A_2$, and only a very

small fraction of the excited ions will decay through this path. This explains why there are no visible R-lines in the emission spectra from Cr^{3+}-ions in crystals with low crystal field strength.[6]

1.1.2   High crystal field strength

In high crystal field strength, the lowest excited state of the Cr^{3+}-ions is the ^2E state, see Figure 2. At low temperatures the emission is dominated by the transition $^2E \rightarrow ^4A_2$ (R-lines), yielding an effective long fluorescence lifetime, since the transition is parity and spin forbidden. The $^4T_2$ state has a much shorter lifetime than the ^2E state. When the temperature increases, a higher percentage of the Cr^{3+}-ions will populate the $^4T_2$ state according to the Boltzmann distribution. Consequently more ions will decay through the $^4T_2 \rightarrow ^4A_2$ path, resulting in a decrease of the fluorescence lifetime. Thus, at low temperatures the thermally activated populations of the ^2E and $^4T_2$ states determine the fluorescence properties. At high temperatures, above 600 K, more ions will be elevated to Q and nonradiative transitions become more significant and will speed up the decay even further.[6]
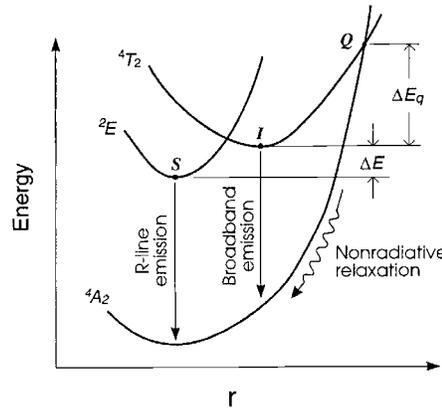
Figure 2. The energy levels as a function of nearest neighbour distance
for a crystal with a high crystal field strength[6]

1.1.3   Temperature sensitivity

Different Cr^{3+}-doped crystals have different temperature dependence of the fluorescence. This leads to a higher sensitivity for temperature changes in some temperature regions. In Figure 3 the temperature dependence on the fluorescence lifetime can be seen for alexandrite, Cr:LiSAF and ruby.[6] As can be seen in the figure, ruby has a very low sensitivity in the temperature region 300 – 400 K. Due to this, ruby was not a strong candidate for this project.
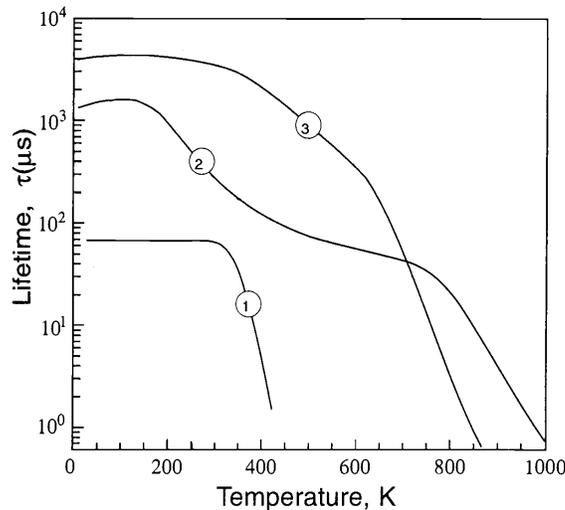
Figure 3. Temperature dependences of the fluorescence lifetime for Cr^{3+}-ions
in different host materials; 1 LiSAF, 2 alexandrite and 3 ruby[6]

1.2 Fluorescence lifetime

The fluorescence lifetime can be measured by using an excitation source whose intensity is modulated by a sinusoidal signal, ν_m. The fluorescence signal will then be forced to follow the same modulation frequency as the excitation source, but lagging with a phase shift, illustrated in Figure 4.[6]

Figure 4. Phase measurement of fluorescence liftetime[6]

The AC fluorescence response signal is then given by (1)

$$\nu_f = V_A \sin(\omega t - \varphi), \qquad (1)$$

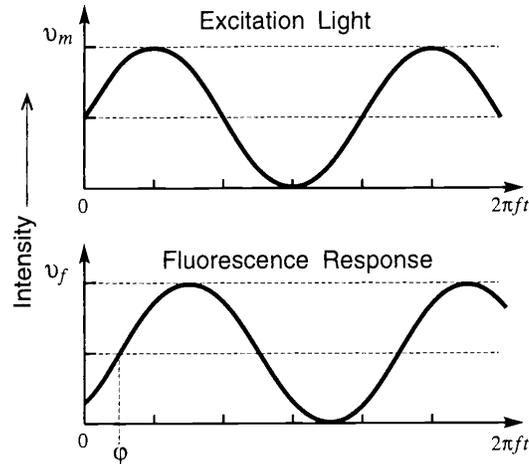where V_A is the amplitude of the fluorescence response signal, ω is the angular frequency of the modulation signal, t is the elapsed time and φ is the phase lag with respect to ν_m. The fluorescence lifetime, τ, is given by (2):[6,8]

$$\tan \varphi = \omega \tau . \qquad (2)$$

2. MATERIAL AND METHODS

In the beginning fluorescence lifetime measurements were performed on small crystals of three different types. Two of the crystals were chosen for further experiments. The crystals were pulverised and attached to a fibre tip with glue. The same experiment was performed again with this configuration. One of these two crystals was selected to make a calibration curve with a more powerful laser used for photodynamic therapy. An experiment was also performed on pork chop as a tissue phantom.

2.1 Fluorescence lifetime measurements of three Cr^{3+}-doped crystals

Three different Cr^{3+}-doped crystals were found to be suitable for the purpose, namely alexandrite, Cr:YAG and Cr:LiSAF. These crystals have sufficient temperature sensitivity in the region 20 – 70 °C and can be excited by light at 635 nm.

2.1.1 Experimental set-up

The measurements were made with the set-up illustrated in Figure 5. The laser used was a He-Ne laser, Latronix, Sweden, emitting light at 632.8 nm with an output power of 2.3 mW. The laser light was focused into a 600 μm core diameter optical quartz fibre (Fiberguide Industries, USA) with the help of a 50 mm focal length lens with a diameter of 25 mm. In the beam path there was a chopper wheel, model SR540 from Stanford Research Systems. The distal end of the fibre was led into an oven, model FN300 Nüve Microprocessor, where the fibre tip was hold in contact with the crystal with the use of a specially designed holder. Here the laser light excited the crystal. The holder was designed to fasten the crystal and to hold up to three fibres in their desired positions.

One detection fibre was fixed in the designed holder, opposite to the fibre from the light source. It collected both the fluorescence light from the crystal and some of the scattered laser light, and guided the light to a photomultiplier tube, model R928 Hamamatsu. Between the fibre tip and the photomultiplier tube there was a holder for optical filters. The holder has two different positions. In one position the filters only let the laser light pass and in the other position only the fluorescence light passes through. The signal from the photomultiplier tube was led to the input channel of a lock-in amplifier, model SR830 from Stanford Research Systems. The photomultiplier tube generated a current signal captured by the lock-in amplifier in the volage mode as the current passed through a resistance of 10 kΩ. A reference signal to the lock-in amplifier was obtained from the chopper wheel. The lock-in amplifier measured the phase difference between the input signal and the reference signal. Another detection fibre was positioned next to the first one. It collected some of the fluorescence induced in the crystal and guided it to an optical multichannel analyzer (OMA) system. This system recorded the fluorescence emission spectrum.

Figure 5. The set-up used to measure the temperature with crystals

Two thermistors were used inside the oven to monitor the temperature changes. The resistance of a semiconductor material is the temperature dependent parameter in a thermistor. The signal from the thermistors was analysed by a computer program, which made it possible to monitor the temperature on a computer screen in real time during the experiments.

The chopper frequency, f, was chosen close to

$$f \sim \frac{1}{2\pi\tau}, \qquad (3)$$

in order to get a good accuracy in the measurement of the fluorescence lifetime.

2.1.2 Experimental description

The crystal was fixed in the holder, which was placed inside the oven. The excitation and detection fibres were inserted into the oven through a hole. The fibres were placed in the holder. The two thermistors were placed in contact with the crystal. The laser was turned on and the oven was heated to the desired temperature. The temperature was monitored on

the computer screen and when it had stabilized a measurement was made. First the fluorescence light was detected and the phase difference between the fluorescence signal and the reference signal was displayed on the lock-in amplifier. Then the filters were shifted so that only scattered laser light could be detected, and the phase difference between the laser signal and the reference signal was displayed. After this the temperature was raised to the next temperature and the procedure was repeated. Measurements were performed until temperatures of about 70 °C were reached. The data recorded at each temperature were the fluorescence emission spectrum, the two phase differences, the both thermistors' temperatures and the chopper frequency. Four separate series of measurements were conducted sequentially for each crystal, to study the reproducibility.

2.1.3   Calculation of fluorescence lifetime

To calculate the fluorescence lifetime, a program in MATLAB was written for each crystal. The two phase differences, the frequency and the temperatures from the thermistors were the input data to the program. The first computation was to calculate the phase difference between the fluorescence and the laser light, with the formula (4):

$$\Delta\varphi = \varphi_{fluorescence} - \varphi_{laser} \qquad (4)$$

The lifetime could then be calculated as (5):[6]

$$\tau = \frac{\tan \Delta\varphi}{2\pi f} \qquad (5)$$

A graph was drawn with the lifetime as a function of temperature including all four series of measurements. The temperature was chosen as a mean value of the two thermistors' temperatures. A polynomial of degree two ($ax^2 + bx + c$) was fitted to the data from the four measurements, with the least squares method. In a new graph a polynomial of degree two was fitted to all the datapoints from the four series. The standard deviation was also calculated for the difference between the data points. The relative standard deviation was calculated as the standard deviation divided by the mean value of the lifetime.

2.2   Characterization of crystal attached to fibre tip

After the initial experiments alexandrite and Cr:LiSAF were chosen for the continuing experiments. The crystals were pulverised in a mortar. One grain of the crystal was glued to the fibre tip using a non-fluorescent epoxy. After curing, a second layer of epoxy was applied around the crystal to minimise the influence of the environment on the fluorescence of the crystal.

2.2.1   Experimental set-up

The experimental set-up was almost the same as in the previous section 2.1.1. The difference was that the crystal was much smaller and glued onto the tip of the fibre, coming from the laser. The fibre used was 400 μm in diameter. A bandpass filter, 630 ± 5 nm, was now placed in front of the laser to filter out unwanted emission of the other wavelengths.

2.2.2   Experimental description

The fibres were inserted into the oven and fastened in the holder and the thermistors were placed as close to the small crystal as possible. The experiment was conducted in the same way as in section 2.1.2. Only two measurement series for each crystal were performed. Calculations were conducted in the same way as in section 2.1.3.

2.3   Fluorescence lifetime measurements on crystals attached to fibre tip with a PDT-laser

After selecting the best suited crystal for our purpose, Cr:LiSAF, the fibre was tested with a more powerful laser, a high power laser normally used for PDT. A new fibre had to be prepared since the first one was broken. In this experiment both the excitation and fluorescence light were guided through the same fibre. With this new set-up a calibration curve was made.

2.3.1 Experimental set-up

The experiment was performed with the set-up seen in Figure 6. The laser was a Ceralas™ PDT635, CeramOptec, diode laser. Since the laser exhibited a broad emission profile from 630 - 700 nm with a peak at 635 nm, a bandpass filter 635 ± 5 nm was inserted in front of the laser, so that no laser light, except 635 nm, could influence the fluorescence measurements. The laser was focused into the fibre with a lens system, which produced a 1:1 image of the object.
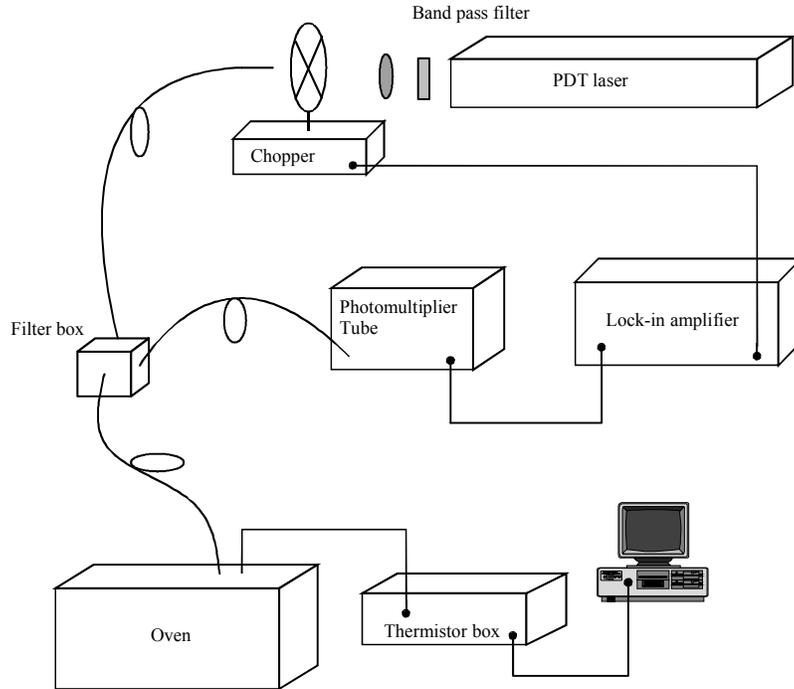

Figure 6. The experimental set-up to make the calibration curve

To be able to excite the crystal and detect the fluorescence light through the same fibre, a small box containing a beamsplitter (50/50) and three fibre connections was used. From one of the connections the laser light is partly transmitted straight through the box into the probe fibre, which leads the excitation light to the crystal. The fluorescence light from the crystal is collected by the same probe fibre and the light is guided back to the filter box. Here the light is partly reflected by the beamsplitter into the third fibre, which leads to the photomultiplier tube.

2.3.2 Experimental description

The lifetime was measured for several temperatures in the same way as in previous experiments, see section 2.1.2. The laser power was adjusted so that 7 mW came out of the fibre with the crystal. The set-up was however optimised for high throughput. After three series of measurements a calibration curve for the fibre was made. The calculations were conducted in the same way as in section 2.1.3.

2.4 Characterization of fibre sensor in in vitro measurements of pork chop

To see if it was possible to measure the temperature with the same accuracy in tissue as in air, an experiment was made on pork chop as a tissue phantom.

2.4.1 Experimental set-up

The set-up is the same as in Figure 6. The fibre tip with the crystal was now placed between two pork chops inside the oven. The thermistors were placed on either side of the fibre, thermistor 1 placed 1 – 2 mm from the fibre and thermistor 2, 5 - 6 mm from the fibre.

2.4.2   Experimental description

The temperature in the oven was raised and when the temperatures measured by the thermistors had stabilized a fluorescence lifetime measurement was performed in the same way as in section 2.1.2. This was repeated until the pork chop reached the temperature of 59 °C. The lifetime was calculated for the different temperatures and was drawn in the same figure as the calibration curve. The lifetime was plotted as a function of temperature of the closest thermistor.

3. RESULTS

3.1   Results of the lifetime measurements of whole crystals of alexandrite, Cr:YAG and Cr:LiSAF

In Figure 7 the lifetime for alexandrite is plotted as a function of temperature. Four different series of measurements are included and the graph shows a good reproducibility.
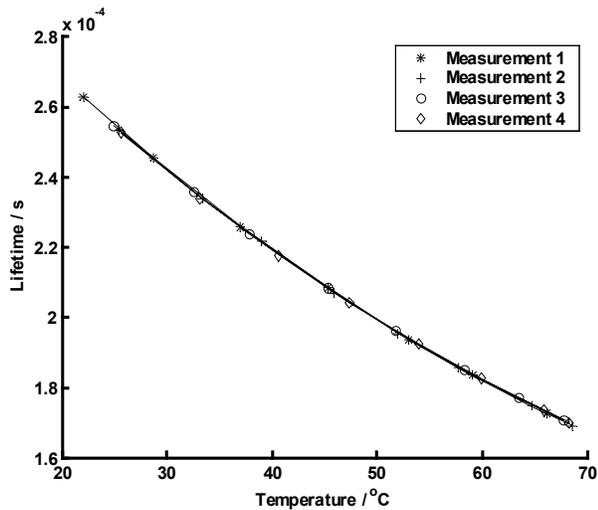

Figure 7. The lifetime as a function of temperature for alexandrite, almost a perfect overlap of the curves indicates a good reproducibility
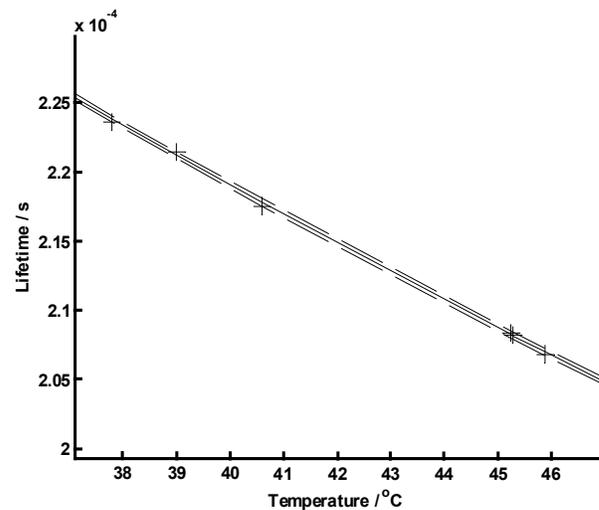
Figure 8. The fitted curve to the four measurements in a narrowed temperature interval for alexandrite, solid line, and the standard deviation, dashed line

The curve fitted to the four measurements and the standard deviation is included in Figure 8. The standard deviation was determined to 2.5 x 10^{-7} s and the relative standard deviation was 0.12 %. Only a fraction of the curve is shown in the graph to make it more readable. The precision in the temperature measurements can be estimated as the standard deviations of specific lifetime readings. The temperature precision for alexandrite can be estimated to ± 0.2 °C in the studied interval.

The measured lifetime for Cr:YAG as a function of temperature is shown in Figure 9. Four different measurements are included and this graph illustrates also a good reproducibility.
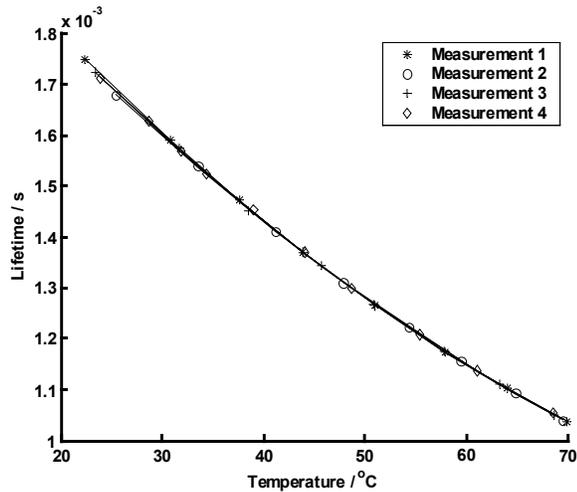

Figure 9. The lifetime as a function of temperature for Cr:YAG. The reproducibility is almost as good as for alexandrite
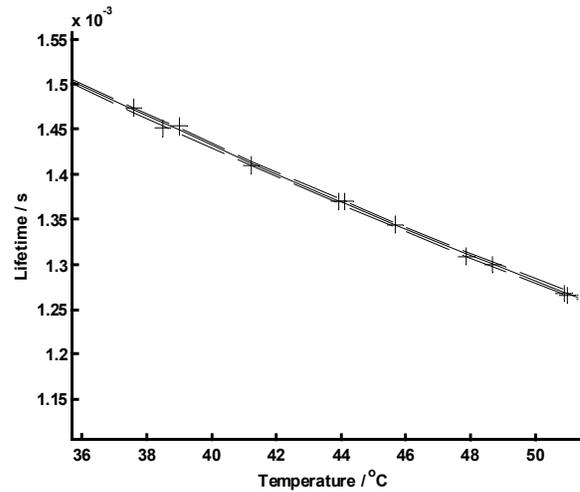

Figure 10. The fitted curve to the four measurements for Cr:YAG, solid line, and the standard deviation (dashed line)

The curve fitted to the four measurements and the standard deviation, 2.7×10^{-6} s are seen in Figure 10. The relative standard deviation was determined to 0.20 %. Only a part of the curve is shown in the graph. The temperature precision of Cr:YAG is approximately ± 0.25 °C.

In Figure 11 the lifetime for Cr:LiSAF is plotted as a function of temperature. Four different measurements are included illustrating the reproducibility.
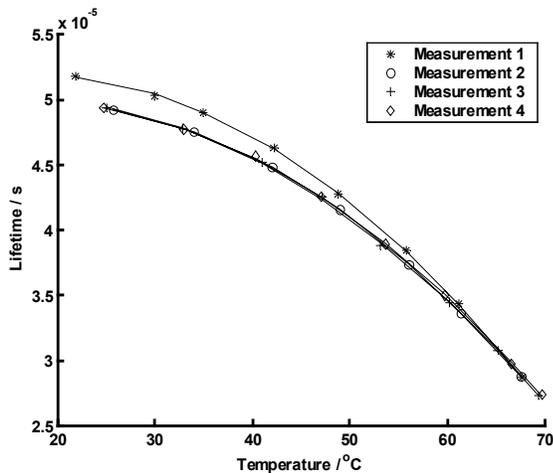

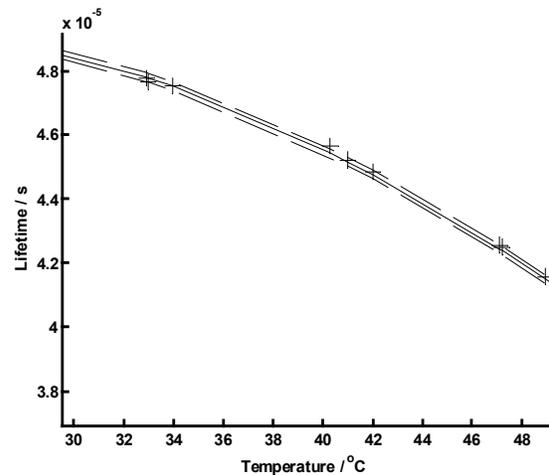Figure 11. The lifetime as a function of temperature for Cr:LiSAF. It also shows the reproducibility

Figure 12. The fitted curve to the three measurements for Cr:LiSAF, solid line, and the standard deviation (dashed line)

The curve fitted to the last three measurements and the standard deviation, 1.4×10^{-7} s is seen in Figure 12. The first measurement was omitted due to its deviation from the others. The relative standard deviation was 0.35 %. Only a part of the curve is shown in the graph. The temperature precision for Cr:LiSAF is estimated to ± 0.3 °C.

3.2 Characterization of crystal attached to fibre tip

The experiments ware repeated for alexandrite and Cr:LiSAF, this time with the crystal fragments glued to fibre tip. The same precision for both crystals was obtained as in section 3.1. The only difference was that there was a slight difference in the calculated values of the lifetimes compared to the ones in section 3.1.

3.3 Fluorescence lifetime measurements on crystals attached to fibre tip with a PDT-laser

The calibration curve for Cr:LiSAF can be seen in Figure 13. The lifetime is plotted versus the temperature, indicating also the standard deviation, 3.2×10^{-7} s. The relative standard deviation was determined to 0.85 %. The corresponding temperature precision is approximately ± 0.5 °C.
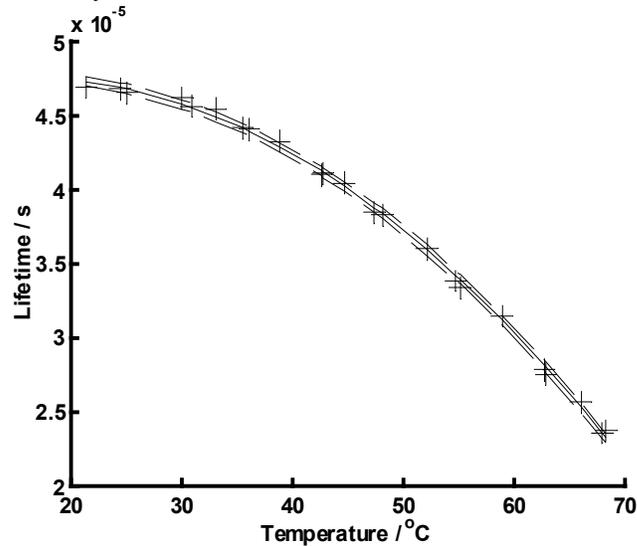

Figure 13. The calibration curve, solid line, for Cr:LiSAF
and standard deviation, dashed line, measured values, +

3.4 Characterization of fibre sensor in in vitro measurements of pork chop

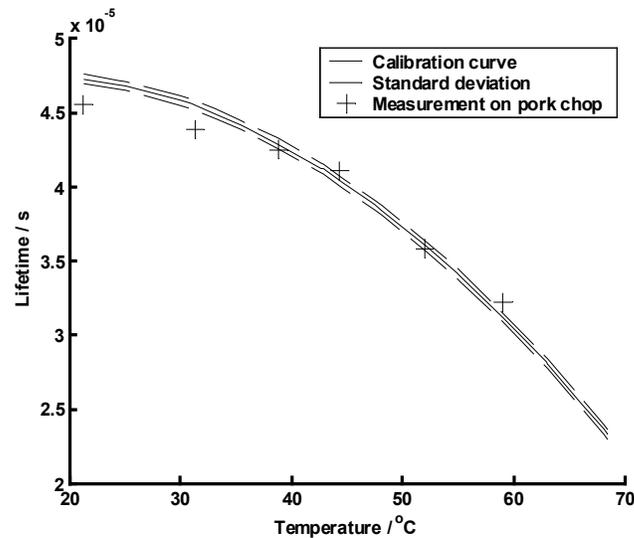Figure 14 shows the calibration curve together with the measurements on the pork chop.

Figure 14. Calibration curve, solid line, and standard deviation, dashed line,
together with the measurements on pork chop, +

4. DISCUSSION AND CONCLUSION

4.1   Fluorescence lifetime measurements of three Cr^{3+}-doped crystals

When comparing the three crystals they all provide a relatively high accuracy, within the estimated limit ± 0.5 °C. Cr:LiSAF exhibit not as high slope between 20 – 25 °C as the other two crystals. However since the temperature during an IPDT treatment is over 30 °C, this has less relevance for some applications. All the crystals have longer lifetimes, µs – ms, than PpIX, which has a lifetime in the nanosecond region. This makes it possible to separate the fluorescence from the crystals from the fluorescence from PpIX in time. For further experiments Cr:YAG was not selected because of the strong fluorescence in the red region, making it impossible to detect other fluorophores, for example PpIX, when monitoring the fluorescence spectrum during an IPDT treatment.

4.2   Characterization of crystal attached to fibre tip

One can see that there is a difference in measured lifetimes, when comparing the results from the previous measurements on a whole crystal with the ones obtained when a small crystal was glued to the fibre tip. This can be due to that the crystal can be warmer than the two thermistors, when they are not in the exact same position as the crystal. The equipment is also very sensitive to the amount of fluorescence intensity. If the intensity is too low, the system becomes unstable, thus showing a too short lifetime. It is important that no laser light is detected together with the fluorescence light, since this will shorten the lifetime obtained. Even a very small amount of laser light can ruin a measurement. It is therefore important to choose optical filters that efficiently block the laser light.

The method to glue the crystal to the fibre is not a good choice. This is due to the difficulty to place the crystal in a position on the fibre tip so that the detected fluorescence intensity is as high as possible. As stated before, only a little decrease in the fluorescence can effect the fluorescence lifetime measurements. Another problem is that the glue does not attach so hard to the fibre, resulting in that the crystal very easily falls off when subjected to mechanical stress. The amount of glue used can also affect the results. Large amount of glue between the fibre and crystal can decrease the amount of fluorescence induced and detected. A better alternative would be to dope the fibre tip with the crystal.

4.3   Fluorescence lifetime measurements on crystals attached to fibre tip with a PDT-laser

The calibration curve was done with a different fibre than the one used in section 4.2, explaining why the calibration curve has different lifetimes. This measurement did not give the same accuracy as our previous results, but it still fulfils the requirements defined for this project. An explanation to the larger deviations can be that the crystal is further away from the fibre tip, resulting in a decrease in fluorescence intensity. This indicates that each fibre made in this way needs to be treated individually and a calibration curve versus known temperatures has to be measured for each fibre. The most important thing is to know which temperature a specific lifetime corresponds to for a specific fibre probe. If this is in agreement with theoretical data is of less importance.

4.4   Characterization of fibre sensor in in vitro measurements of pork chop

In Figure 14 one can see that the lifetime measurements on pork chop give a shorter fluorescence lifetime than expected for lower temperatures. The results for higher temperatures follow the calibration curve better. This can be interpreted as, for lower temperatures the laser light also heats the crystal, but at higher temperatures this heating process becomes negligible.

4.5   Future developments

This preliminary study indicates that this type of fibre probes could be used for measurements of local tissue temperatures in connection with laser therapy. Since the intensity of the fluorescence has been sufficient in these preliminary and unoptimized measurements using low laser power, it should not be any problem to use much smaller crystals than has been used here. Our suggestion is therefore to "dope" the fibre ends with miniature crystals. It is important that such fibre tip will not absorb too much of the treatment light, or it will decreace the therapeutic effect and act as a local heat source. One could further consider the concept suggested by Lilge et al. to use a single fibre probe measuring at several positions along the fibre.

REFERENCES

1. Dougherty TJ, Thoma RE, Boyle DG, Weishaupt KR. Interstitial photoradiation therapy for primary solid tumors in pet cats and dogs. Cancer Res 1981; 41: 401- 404.

2. Marijnissen JPA, Versteeg JAC, Star WM, van Putten WLJ. Tumor and normal response to interstitial photodynamic therapy of the rat R- 1 rhabdomyosarcoma. Int J Radiat Oncol Biol Phys 1992; 22: 963 - 972.

3. Sturesson, C. "Medical Laser-Induced Thermotherapy - Models and Applications." Diss. Lund Institute of Technology, 1998.

4. af Klinteberg, C. "On the Use of Light for the Characterization and Treatment of Malignant Tumours." Diss. Lund Institute of Technology, 1999.

5. Johansson, T. et al. "Feasibility study of a novel system for combined light dosimetry and interstitial photodynamic treatment of massive tumors." Applied Optics 41.7 (2002): 1462-68.

6. Grattan, K. T. V. and Z. Y. Zhang. Fiber Optic Fluorescence Thermometry. 1 ed. London: Chapman & Hall, 1995.

7. Powell, R. C. et al. "Spectroscopic properties of alexandrite crystals." Physical Review B 32.5 (1985): 2788-97.

8. Armstrong, L and S Ferneuille. "Theoretical analysis of the phase shift measurement of lifetimes using monochromatic light." Journal of Physics B 8 (1975): 546.